Free radicals formed by H(Mu) addition to fluoranthene

Jean-Claude Brodovitch, Brenda Addison-Jones, Khashayar Ghandi, Iain McKenzie, Paul W. Percival, and Joachim Schüth

Abstract: Muonium has been used as an H atom analogue to investigate the free radicals formed by H addition to the polyaromatic hydrocarbon fluoranthene. There are nine unique carbons in the molecule, but only five radicals were detected. Muon and proton hyperfine constants were determined by transverse field µSR and µLCR, respectively, and compared with calculated values. All signals were assigned to radicals formed by Mu addition to C-H sites. There is no evidence for addition to the tertiary carbons at ring junctions.

Key words: muonium, fluoranthene, free radical, hyperfine constants.

Résumé : Les radicaux libres formés par addition de l'atome d'hydrogène à la molécule aromatique du fluoranthène ont été étudiés en utilisant le muonium comme analogue de l'atome d'hydrogène. Il y a neuf carbones non-équivalents présents dans la molécule, toutefois, seulement cinq radicaux libres ont été détectés. Les constantes hyperfines du muon et de certains des protons ont pu être déterminées par spectroscopies µSR et µLCR et les valeurs obtenues ont été comparées à des valeurs calculées. Tous les signaux observés ont pu être attribués aux radicaux libres formés par l'addition de Mu aux carbones portant le groupe C-H; l'addition de Mu aux carbones tertiaires qui joignent les cycles aromatiques ne se fait pas.

Mots clés : muonium, fluoranthène, radicaux libres, constantes hyperfines.

Introduction

One of the interesting questions raised in the past decade of research on fullerenes is how reactivity to radical attack is influenced by curvature of a carbon skeleton (1–3). Consider the addition of a single H atom or other small radical to C_{60} and to C_{70}. In the former case there is only one possible radical product, since all carbons are identical. In contrast, the ellipsoidal C_{70} has five chemically inequivalent sets of carbon atoms, and therefore five distinct radicals could be formed. Of these, the least reactive is the carbon at the "equator" where the curvature is least. Since high reactivity is associated with release of strain energy at a site of high curvature (1), it follows that planar carbon sites would be least reactive.

To test the reactivity of "flat" polyaromatic hydrocarbons (PAHs) we investigated Mu or H atom addition to pyrene, whose carbon skeleton can be considered a fragment of C_{70} (4). Three radicals were identified, but all are formed by Mu addition to secondary carbons at the edge of the molecule, in the same way that cyclohexadienyl is formed by H or Mu addition to benzene. No evidence was found for addition at the tertiary carbon sites that most resemble those of a fullerene.

The present study is an extension of our investigation to fluoranthene (Fig. 1). Although the PAH itself is planar, its carbon skeleton is a common fragment of fullerenes where isolated five-membered rings are surrounded by 6-rings. Since this feature introduces curvature to a fullerene, its presence might promote radical addition at ring junctions in PAHs.

As far as we know there is no literature data on monohydrofluoranthene radicals.

Muon spin rotation and muon level-crossing resonance experiments

Experiments were performed at the M20 muon beam line of the TRIUMF cyclotron facility in Vancouver, BC. The sample was pure fluoranthene sealed oxygen-free in a stainless steel vessel fitted with a thin steel foil window. Its temperature was maintained at ≈ 117°C (above the melting point of fluoranthene) by passing fluid from a constant temperature bath (set at 120°C) through the sample mount, which was surrounded by vacuum. A liquid sample was needed to ensure sharp spectral features by averaging anisotropic hyperfine parameters. The alternative to a neat liquid is to use a solution, as in the previous study (4), but this generally leads to less intense radical signals, as a fraction of the incident muons end up in the solvent.

Transverse field muon spin rotation (µSR) and muon (avoided) level-crossing resonance (LCR) spectra were accumulated over a period of several days. Apart from the higher

Received 18 October 2002. Published on the NRC Research Press Web site at http://canjchem.nrc.ca on 14 January 2003.

J.-C. Brodovitch, B. Addison-Jones, K. Ghandi, I. McKenzie, P.W. Percival,[1] and J. Schüth.[2] Department of Chemistry and TRIUMF, Simon Fraser University, Burnaby, BC V5A 1S6, Canada.

[1] Corresponding author (e-mail: percival@sfu.ca).

[2] Present address: debis Systemhaus Information Security Services GmbH, Rabinstrasse 8, 53111 Bonn, Germany.

doi: 10.1139/V02-191

Fig. 1. The fluoranthene molecule and the IUPAC numbering system used in this paper.

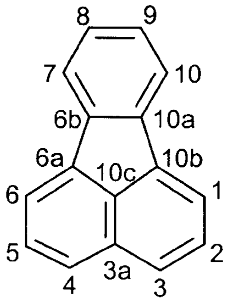

Fig. 2. Part of the Fourier power μSR spectrum from liquid fluoranthene at 118°C in an applied magnetic field of 17.34 kG. The peaks labeled **1**–**5** are due to free radicals formed by Mu addition to different sites in the fluoranthene molecule.

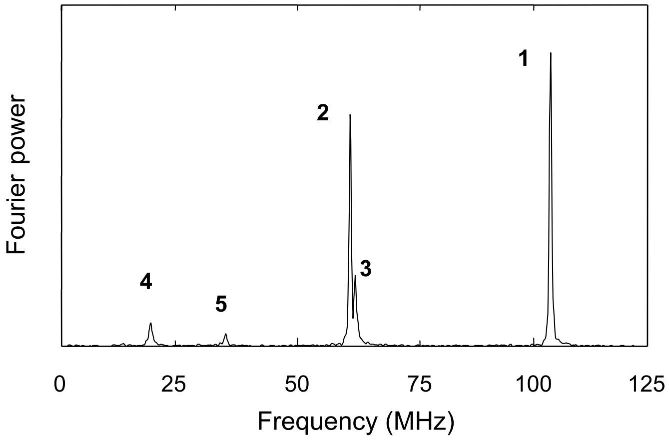

Fig. 3. Muon level-crossing resonance spectrum from liquid fluoranthene at 117°C.

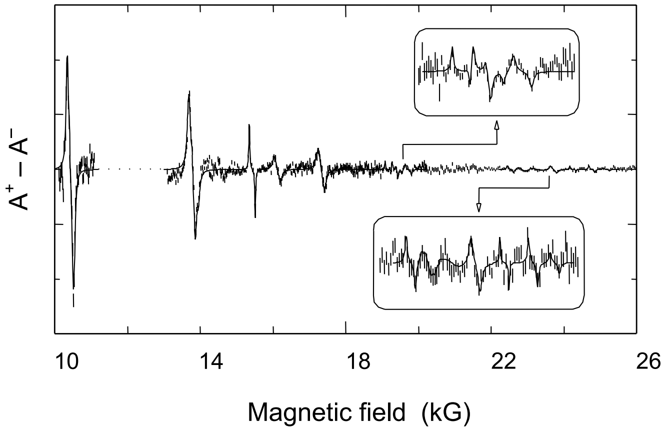

Table 1. Measured muon hyperfine constants for the five observed Mu-fluoranthenyl radicals and their relative abundance derived from μSR signal amplitudes.[a]

Radical	A_μ (MHz)	Abundance (%)
1	263.87(1)	35.8(7)
2	348.95(2)	26.8(7)
3	347.35(3)	14.2(7)
4	434.86(5)	13.7(6)
5	402.25(6)	9.5(1.1)

[a] Statistical uncertainties are shown in parentheses.

temperature, the apparatus and measurement procedures were as described previously (4). Spin-polarized positive muons (4 MeV) were extracted from the beam line and stopped in the sample, which was mounted in the HELIOS μSR spectrometer whose magnetic field was aligned along the beam direction. Transverse muon polarization was used for the μSR measurements and longitudinal polarization for LCR, with the positron counters arranged accordingly (4). Figure 2 shows an example of a μSR spectrum at a fixed magnetic field, 17.34 kG. The LCR spectrum displayed in Fig. 3 is a composite of many individual runs over different field ranges. Repeated runs were needed to achieve acceptable signal-to-noise for the weakest signals.

The signals of five radicals are evident in the transverse field μSR spectra; two of them are almost degenerate (close to 60 MHz in Fig. 2). Although each radical gives rise to a pair of muon precession frequencies (ν_{R1} and ν_{R2}; see eq. [1] below), only the lower frequency signals are visible in the range displayed in Fig. 2. (Their higher frequency partners are less intense, mainly because of the limited time resolution of the apparatus.) Measurements at different magnetic fields confirmed the assignment of the signals to muoniated radicals. Their muon hyperfine constants (A_μ) were calculated from theoretical expressions for the precession frequencies (4, 5)

$$[1] \qquad \nu_{R1} = \nu_{mid} - \frac{1}{2}A_\mu \qquad \text{and} \qquad \nu_{R2} = \nu_{mid} + \frac{1}{2}A_\mu$$

where

$$[2] \qquad \nu_{mid} = \tfrac{1}{2}\left[\sqrt{A_\mu^2 + (\nu_e + \nu_\mu)^2} - \nu_e + \nu_\mu\right]$$

and ν_e and ν_μ are the electron and muon Larmor frequencies.

The results are summarized in Table 1, which also lists the relative abundances of the five radicals as determined from the signal amplitudes. In principle, nine different radicals could be formed by Mu addition to fluoranthene, since there are nine unique carbons (1, 2, 3, 7, 8, 10a, 10b, 10c, and 3a; all but the last two are doubly degenerate; see Fig. 1). Assignment of the μSR signals to specific radical structures is not possible without further information, so at this stage they are simply labeled **1**–**5** in decreasing order of intensity.

Interpretation of the LCR spectrum (Fig. 3) is more complicated. Each of the five radicals detected by μSR will also have hyperfine interactions between the unpaired electron and the protons in the molecule. Since fluoranthene has ten protons, each muoniated radical could potentially give rise to ten LCR resonances, with the signals from different radicals distributed in overlapping field regions. In practice only the largest proton couplings are likely to give detectable signals, and the LCR signals will also be scaled by the radical abundances (Table 1). Up to 17 resonances can be distinguished in Fig. 3. Their differential-like shape is a result of square-wave modulation of a small component of the ap-

Table 2. Fitted parameters of muon level-crossing resonances detected for Mu-fluoranthenyl radicals.

Field (kG)	Width (G)	Relative amplitude
10.434(1)	38(2)	1.00
13.771(1)	53(2)	0.60(2)
13.867(3)	42(5)	0.18(2)
15.4272(5)	15.4(7)	0.38(1)
16.120(4)	57(7)	0.11(8)
17.325(5)	70(14)	0.18(2)
19.161(2)	13(3)	0.067(8)
19.349(2)	20(4)	0.077(8)
19.466(4)	17(8)	0.033(8)
19.721(4)	24(6)	0.042(6)
22.819(34)	45(19)	0.013(7)
23.717(7)	46(14)	0.03(4)
24.246(6)	11(8)	0.03(2)
24.771(7)	24(11)	0.026(8)

plied magnetic field, which is used to suppress some of the baseline fluctuations (4). The resonances were fitted with a Lorentzian line shape; the fit parameters for the strongest 14 are gathered in Table 2. The few extra features that could not be fitted with physically meaningful parameters are barely above the noise and were ignored in the final analysis.

For protons, the resonance field is given by (4,5)

$$[3] \qquad B_{\mathrm{LCR}} \approx \frac{1}{2}\left[\frac{A_\mu - A_\mathrm{p}}{\gamma_\mu - \gamma_\mathrm{p}} - \frac{A_\mu + A_\mathrm{p}}{\gamma_\mathrm{e}}\right]$$

where A_p is the proton hyperfine constant (hfc) and γ_μ, γ_p, and γ_e are the magnetogyric ratio of the muon, proton, and electron, respectively. In addition, the width and the amplitude of a resonance are given by

$$[4] \qquad \mathrm{Width} = \frac{1}{2}\,\frac{\sqrt{\omega_{\mathrm{LCR}}^2 + \lambda_{\mathrm{eff}}^2}}{\pi(\gamma_\mu - \gamma_\mathrm{p})}$$

$$[5] \qquad \mathrm{Amplitude} \propto \frac{\omega_{\mathrm{LCR}}^2}{\omega_{\mathrm{LCR}}^2 + \lambda_{\mathrm{eff}}^2}$$

where ω_{LCR} is the frequency at resonance and λ_{eff} the effective relaxation rate (muon decay rate plus any additional relaxation contribution),

$$[6] \qquad \omega_{\mathrm{LCR}} = \frac{\sqrt{c}\,\pi A_\mu A_\mathrm{p}}{\gamma_\mathrm{e} B_{\mathrm{LCR}}}$$

and c is the number of magnetically equivalent protons at resonance.

Clearly, to calculate the hyperfine constant of a particular proton from its resonance field position (B_{LCR}) it is necessary to know the value of the muon hfc (A_μ) for that particular radical. Thus, the first step in assigning the LCR resonances is to deduce which resonances correspond to which A_μ values. Our experience interpreting the LCR spectrum of muoniated pyrenyl isomers was beneficial, and following the procedure described in ref. (4) we identified five resonances due to the –CHMu– group. As indicated in Table 3, the ratio of muon and proton hfcs is in the range 1.20–1.25 after correction for the different magnetic moments (correction factor = 3.183). This muon–proton isotope effect is typical for cyclohexadienyl type radicals and is consistent with zero-point vibrational effects in anharmonic vibrational modes (5, 6).

Table 3. Assignment of muon level-crossing resonances due to methylene (–CHMu–) groups in Mu-fluoranthenyl radicals.

Field (kG)	Assignment	A_μ (MHz)	A_p (MHz)	$(A_\mu/A_\mathrm{p})/3.183$
10.434(1)	**1**	263.87(1)	68.81(2)	1.20
13.771(1)	**2**	348.95(2)	91.50(3)	1.20
13.867(3)	**3**	347.35(3)	88.13(6)	1.24
16.120(4)	**5**	434.86(5)	111.01(10)	1.23
17.325(5)	**4**	402.25(6)	100.93(9)	1.25

Table 4. Relative energies of formation and muon hfcs calculated for the nine possible fluoranthenyl radicals, compared with the experimental muon hfcs and the radical assignment.

Mu site	ΔE (kJ mol^{-1}) [a]	A_μ(calcd.) (MHz)[a,b]	A_μ(exptl.) (MHz)	Radical
C-3	0	278	264	**1**
C-1	17	346	347	**3**
C-8	35	355	349	**2**
C-2	42	394	402	**5**
C-7	43	430	435	**4**
C-6a	58	441	—	—
C-6b	72	498	—	—
C-10c	107	732	—	—
C-3a	139	893	—	—

[a] Single point UB3LYP/6–31G** on UB3LYP/STO-3G optimized geometry.

[b] Includes a factor of 1.20 to account for the primary isotope effect.

The remaining resonances from Table 2 are narrower than those assigned to the methylene groups and can be attributed to α protons (protons attached to a carbon that carries significant unpaired spin density). Beyond that one must turn to theoretical prediction to help in the assignment.

Computation and discussion

Model calculations were performed on the nine isomeric H atom adducts of fluoranthene using density functional theory (DFT) as implemented in the Gaussian suite of programs (7). The structures were optimized at the UB3LYP/STO-3G level, and then single-point computations were performed at the UB3LYP/6–31G** level to calculate the hyperfine constants and Hartree–Fock energies.

The molecular geometry for each H adduct radical should also be valid for the muoniated species, within the Born–Oppenheimer approximation. Similarly, electron distributions should be identical for isotopomers. However, zero-point vibrational effects are larger for normal modes involving Mu, and this can result in considerable isotope effects on vibrationally averaged hyperfine interactions. In particular, such effects have been investigated for cyclohexadienyl (6) and HC_{60} (8). In view of the preliminary assignments and hfc ratios indicated in Table 3 we scaled computed proton hfcs by a factor of 1.20 to predict the muon hfc (a factor of

Table 5. Comparison between calculated[a] and experimental muon and proton hfcs (in MHz) for the five assigned Mu-fluoranthenyl radicals (Mu-FA). The experimental proton hfcs were determined from eq. [3] and are listed in order of the corresponding level-crossing resonances.

		1 (3-Mu-FA)		**2** (8-Mu-FA)		**3** (1-Mu-FA)		**4** (7-Mu-FA)		**5** (2-Mu-FA)	
Nucleus	Site	Calcd.	Exptl.	Calcd.	Exptl.	Calcd.	Exptl.	Calcd.	Exptl.	Calcd.	Exptl.
Mu	…	278[b]	263.87	355[b]	348.95	346[b]	347.35	430[b]	434.86	394[b]	402.25
H	C3	68.8[c]	68.81(2)	…	…	…	…	…	…	…	…
H	C8	…	…	87.4[c]	91.50(3)	…	…	…	…	…	…
H	C1	…	…	…	…	85.4[c]	88.13(6)	…	…	…	…
H	C2	–31.2	–23.70(1)	…	…	…	…	…	…	…	…
H	C2	…	…	…	…	…	…	…	…	97.1[c]	100.93(9)
H	C7	…	…	…	…	…	…	105.9[c]	111.01(10)	…	…
H	C2 C8	…	…	…	…	–9.3 –10.8	–9.93(5)[d]	…	…	…	…
H	C5 C10	…	…	…	…	–14 –11.1	–13.43(4)[d]	…	…	…	…
H	C7	…	…	–19.9	–14.00(8)	…	…	…	…	…	…
H	C9	…	…	–27.7	–18.74(7)	…	…	…	…	…	…
H	C6 C4	…	…	…	…	…	…	…	…	–18.8 –17.0	–23.2(6)[d]
H	C3	…	…	…	…	…	…	…	…	–47.9	–39.8(1)
H	C8	…	…	…	…	…	…	–22.8	–17.22(12)	…	…
H	C10	…	…	…	…	…	…	–31.6	–26.94(14)	…	…

[a] Single point UB3LYP/6–31G** on UB3LYP/STO-3G optimized geometry.
[b] Includes a factor of 1.20 to account for primary isotope effect.
[c] Includes a factor of 0.94 to account for secondary isotope effect.
[d] Accidentally doubly degenerate (see text).

3.183 is also required to account for the magnetic moment). Similarly, taking account of prior experience (4), we used a factor of 0.94 for the corresponding H in a –CHMu– group.

The relative Hartree–Fock energies of the nine H adduct radical isomers are listed in Table 4 together with the corresponding predicted muon hfcs. The hfcs of the first five entries (lowest energies) are well matched to the experimental data, although one cannot exclude the H adduct to carbon 6a on this ground alone. The radicals were thus assigned as in the last column of Table 4. It is significant that, as in the case of pyrene (4), only products of attack at H-bearing carbons are experimentally detected. Otherwise, we would have found a muon hfc without a corresponding –CHMu– proton; Table 3 shows that this was not the case.

The calculations also provide the hfc of each proton for each radical species. Using eqs. [3–6], the LCR field, width, and amplitude (weighted with the radical abundance) of the corresponding signals may be predicted. It is then possible to test if the calculated hfc values are found to be a reasonably close match with experimental data obtained after making an a priori assumption of the muon hfc to use for each level-crossing resonance. The results of our analysis are displayed in Table 5.

In this fashion most of the observed LCR signals were assigned, although ambiguity and inconsistency remain for some of the weaker features observed. For example, in the case of the Mu-1-fluoranthenyl radical (radical **3**), calculations predict four negative hfcs for protons in positions 2 (–9.3 MHz), 8 (–10.8 MHz), 5 (–14.1 MHz), and 10 (–11.1 MHz). Experimentally, in the expected field region only two LCR resonances are observed (at 19.35 kG and 19.47 kG), from which one derives proton hfcs of –9.93 MHz and –13.43 MHz. A good fit is obtained if it is assumed that each of these resonances is actually accidentally doubly degenerate, which suggests that protons in positions 2, 8 and 5, 10 have, pairwise, very close hfcs not quite reproduced by the calculations.

Conclusions

Five muoniated radicals (out of the possible nine) are formed by the addition of muonium to fluoranthene. Using DFT calculations as guides for the assignment of the various experimental spectral features, the hyperfine constants of the muon and selected protons in the various radicals could be obtained. The results are summarized in Fig. 4, in which all the assigned hfcs are shown on the structure diagrams for the radicals detected. Unlike the situation for C_{60} or C_{70}, there is no evidence of a radical being formed by Mu attack on one of the trigonal carbon sites (positions 3a, 6a/10b, 6b/10a, 10c), although calculations suggest that an attack at position 6a/10b might be possible.

From the hyperfine constants of the α-protons obtained experimentally, it is also possible to deduce the distribution of unpaired π-spin density ρ_α on the corresponding carbon using McConnell's relation (9)

$$[7] \quad A_H = Q_\alpha \rho_\alpha, \text{ where } Q_\alpha \approx -75 \text{ MHz}$$

The results are displayed in schematic form in Fig. 5. For clarity, only positive spin densities are displayed. Since the experimental data reported here give no *direct* information on carbon atoms not bearing a hydrogen (such information could be obtained from experiments on ^{13}C enriched fluoranthene), the corresponding unpaired spin density displayed

Fig. 4. Assigned hyperfine constants (in MHz) for the five fluoranthenyl radicals. Alternative assignments or degenerate values for radicals **3** and **5** are shown by question marks.

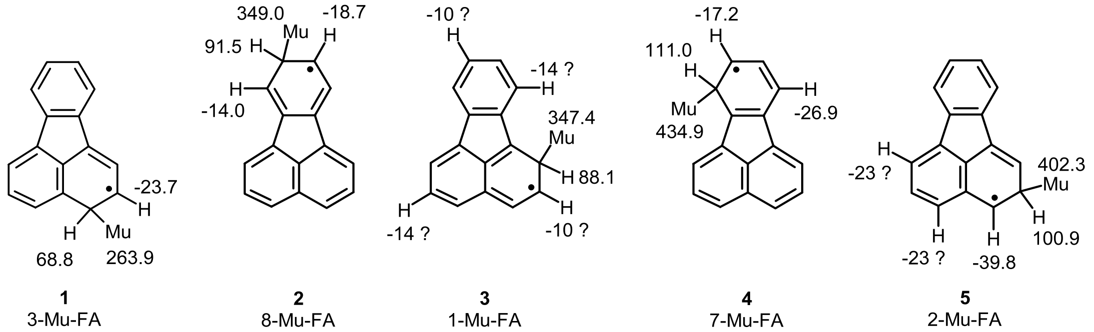

Fig. 5. Principal sites of positive unpaired π-spin density in the five muoniated fluoranthenyl radicals detected. The circled areas are proportional to the spin density as determined from calculations and confirmed from experimentally determined proton hyperfine constants (shaded areas).

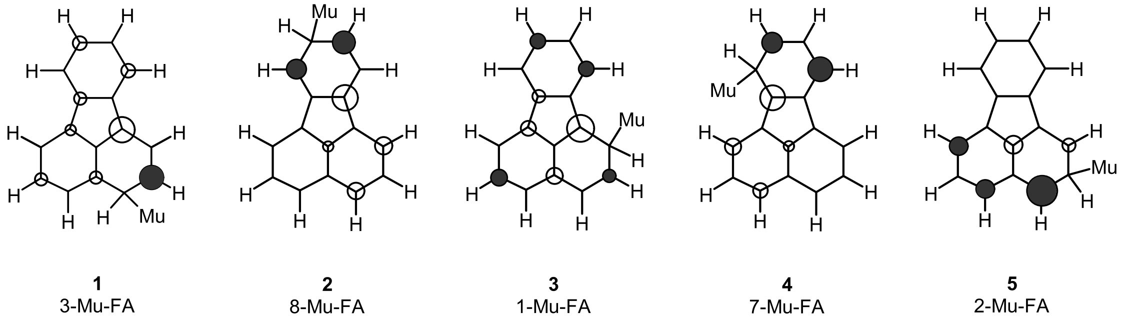

in Fig. 5 was taken from the calculations. It is apparent that most of the protons adjacent to significant unpaired spin density have been detected in the present experiment. However, the calculations seem to indicate that there is significant unpaired spin density on carbons 1 and 3 of radical **2** and carbons 4 and 6 of radical **4**, and that the corresponding proton hfcs may be measurable. In addition, there are a few cases where negative spin density may be sufficient to give rise to measurable *positive* α-proton hfcs.

It is evident from Fig. 5 that radical **1**, the lowest energy isomer, is also the one with the greatest spread of unpaired π-spin density, consistent with a general notion of resonance stabilization. However, it would be dangerous to infer much from the apparent correlation between A_μ and radical energy (Table 4), since other factors contribute to both the relative energies of the radicals and to the muon hfc. In particular, the hfc depends on geometric factors (the dihedral angle between the C—Mu bond and the *z*-axis of the π-spin system) and the unpaired spin density on the adjacent carbon atoms (10, 11).

Similarly, the fact that the lower energy radicals were detected and not those corresponding to Mu(H) addition at trigonal carbon sites is related to the energy required to distort the carbon skeletons of the latter. However, it is important to realize that the relative abundance of the radical isomers depends on *kinetic* competition for the various sites, and that this reactivity is determined by the *activation* energy for Mu(H) addition, which is only indirectly linked to the radical (product) energy.

The findings reported in this paper and the preceding study of Mu addition to pyrene (4) show that planar PAHs are not good models to investigate the reactivity of fullerene fragments. Therefore, as the next stage in our exploration of this topic we have undertaken a study of Mu addition to a pyrenophane, a PAH with a curved carbon skeleton (12).

Acknowledgments

We thank the staff of the TRIUMF μSR Facility for technical support. This research was financially supported by the Natural Sciences and Engineering Research Council of Canada (NSERC) and, through TRIUMF, by the National Research Council Canada (NRC). J. Schüth was the recipient of a NATO postdoctoral fellowship administered by DAAD (Deutscher Akademischer Austauschdienst).

References

1. R.C. Haddon. Science (Washington, D.C.), **261**, 1545 (1993).
2. F. Diederich and C. Thilgen. Science (Washington, D.C.), **271**, 317 (1996).
3. A. Hirsch. *In* Fullerenes and related structures: Topics in current chemistry. Vol. 199. *Edited by* A Hirsch. Springer-Verlag, Berlin. 1999. pp. 1–65.
4. P.W. Percival, B. Addison-Jones, J-C. Brodovitch, K. Ghandi, and J. Schüth. Can. J. Chem., **77**, 326 (1999).
5. E. Roduner. The positive muon as a probe in free radical chemistry: Lecture notes in chemistry. No. 49. Springer-Verlag, Berlin. 1988.
6. D. Yu, P.W. Percival, J.C. Brodovitch, S.K. Leung, R.F. Kiefl, K. Venkateswaran, and S.F.J. Cox. Chem. Phys. **142**, 229 (1990).

7. M.J. Frisch, G.W. Trucks, H.B. Schlegel, G.E. Scuseria, M.A. Robb, J.R. Cheeseman, V.G. Zakrzewski, J.A. Montgomery, R.E. Stratmann, J.C. Burant, S. Dapprich, J.M. Millam, A.D. Daniels, K.N. Kudin, M.C. Strain, O. Farkas, J. Tomasi, V. Barone, M. Cossi, R. Cammi, B. Mennucci, C. Pomelli, C. Adamo, S. Clifford, J. Ochterski, G.A. Petersson, P.Y. Ayala, Q. Cui, K. Morokuma, D.K. Malick, A.D. Rabuck, K. Raghavachari, J.B. Foresman, J. Cioslowski, J.V. Ortiz, B.B. Stefanov, G. Liu, A. Liashenko, P. Piskorz, I. Komaromi, R. Gomperts, R.L. Martin, D.J. Fox, T. Keith, M.A. Al-Laham, C.Y. Peng, A. Nanayakkara, C. Gonzalez, M. Challacombe, P.M.W. Gill, B.G. Johnson, W. Chen, M.W. Wong, J.L. Andres, M. Head-Gordon, E.S. Replogle, and J.A. Pople. 1998. Gaussian 98 [computer program]. Revision A.1. Gaussian, Inc., Pittsburgh, PA.
8. J.R. Morton, F. Negri, and K.F. Preston. Phys. Rev. B. **49**, 12446 (1994).
9. H.M. McConnell. J. Chem. Phys. **24**, 764 (1956).
10. D. Whiffen. Mol. Phys. **6**, 223 (1963).
11. P.W. Percival and S. Wlodek. Chem. Phys. Lett. **196**, 317 (1992).
12. G.J. Bodwell, J.N. Bridson, T.J. Houghton, J.W.J. Kennedy, and M.R. Mannion. Angew. Chem. Int. Ed. Engl. **35**, 1320 (1996).